INTERNATIONAL JOURNAL OF
COASTAL, OFFSHORE & ENVIRONMENTAL ENGINEERING IJCOE Vol.10/No. 4/ Autumn 2025 (19-27)

Available online at: www. Ijcoe.org

Numerical Investigation on Dynamics of DeepCWind Floating Offshore Wind Turbine (FOWT) Platform

Mohammad Ahmadi1, Mahdi Yousefifard2, Hashem Nowruzi3*

1MSc student, Mechanical Engineering Department, Babol Noshirvani University of Technology; mohammad.ahmadih2r@gmail.com

2 Assistant professor,Mechanical Engineering Department, Babol Noshirvani University of Technology; yousefifard@nit.ac.ir

*3*Assistant professor, Mechanical Engineering Department, Babol Noshirvani University of Technology; h.nowruzi@nit.ac.ir*

ARTICLE INFO

Article History:
Received : 17 Apr 2025
Accepted : 06 Jan 2026

Keywords:
FOWT
CFD
Heave and pitch motions
FPSO
OpenFOAM

ABSTRACT

Renewable energies are a crucial component of sustainable development. Offshore wind energy is an interesting clean energy alternative to fossil fuels. In floating offshore wind turbines (FOWTs), a lower floating platform couples/integrates with the upper wind turbine, and the motion of each component influences the other. Therefore, understanding the dynamic behaviors of FOWT platforms is necessary for designing them in real sea states. The present paper numerically investigates the heave and pitch dynamic motions of the DeepCWind FOWT platform at three different offsets between the columns, all under regular waves. To this accomplishment, a 3D RANS-VOF model is implemented in the open-source CFD platform of OpenFOAM. The current numerical simulations of heave and pitch motions of the sandglass-type platform with appropriate accordance are validated against the existing experimental data. The main results show that increasing the offsets between the FOWT platform columns (wide model) significantly reduces the heave and pitch motions. However, the effects of decreasing the distance between the columns (i.e., a tight model) on heave and pitch motions are insignificant compared to the original model.

1. Introduction

Emphasizing renewable energy is a crucial aspect of sustainable development. Consequently, there exists an unequivocal necessity to innovate technologies for the production of renewable energy [1]. The advancement of solar and onshore wind energy has demonstrated considerable efficacy in electricity generation, positioning these sources in competition with conventional production methods such as coal, gas, fuel, and nuclear energy [2]. Recently, despite comprising merely 0.3% of global electricity generation, the growth of offshore wind energy has emerged as a significant enhancement to the energy mix. Offshore wind energy enables the deployment of larger turbines compared to onshore turbines and benefits from a more consistent and robust wind resource, achieving a capacity factor of 40-50% [3]. The International Energy Agency (IEA) reports that offshore wind energy has the potential to satisfy global energy demand 11 times by 2040. To attain this capacity, it is essential to expand installations to deeper water depths. Fixed offshore platforms possess depth constraints.

Consequently, the resolution for utilizing the extensive wind resources of the oceans at greater depths is to transition from fixed platforms to floating structures. The initiation and progression of extensive commercial floating wind projects necessitates enhanced knowledge of turbine power generation. A significant technological challenge in floating offshore wind turbines (FOWTs) is the dynamic behavior of the platform, which induces additional rotor movement and may influence the average power output over time, thereby impacting electricity generation [4]. Consequently, the design of a floating support platform with enhanced dynamic motion may optimize the aerodynamic efficiency of the FOWT. Currently,

prevalent support structures have been established, categorized into four primary types: spar-buoy, tension-leg platform (TLP), semi-submersible, and barge. Each category of these structures employs one of three methods—weights, mooring lines, buoyancy, or a combination thereof—to attain static stability. For a more thorough assessment, one may consult [5]. The semi-submersible platform represents a highly advanced concept in this sector, predominantly utilized in the oil and gas industry, and it appears to possess a marginal advantage in the market for floating offshore wind turbines. This technology predominantly obtains its stability from buoyancy. These platforms possess a considerable advantage due to their catenary anchor lines being more economical than TLP, along with a comparatively simpler installation process. The turbine can be positioned adjacent to the dock, and the floating structure may be towed to its site or returned to shore for maintenance or decommissioning. The primary constraint is its intricate geometry, which complicates construction. This necessitates a considerable quantity of structural mass [6]. The most sophisticated initiative in this category is the WindFloat concept, developed by Principle Power (PP) [7]. In 2011, Principle Power (PP) successfully installed a prototype in Portugal, operated it for four years, decommissioned it, and then reinstalled it in Scotland in 2018. Globally, companies are developing numerous commercial-scale wind farm projects using Windfloat technology. Other companies have introduced semi-submersible concepts at a stage that precedes development. Figure 1 depicts several of them. The research community extensively utilizes the open-source semi-submersible design, DeepCWind, to enhance comprehension of the physics of FOWT and to communicate findings.

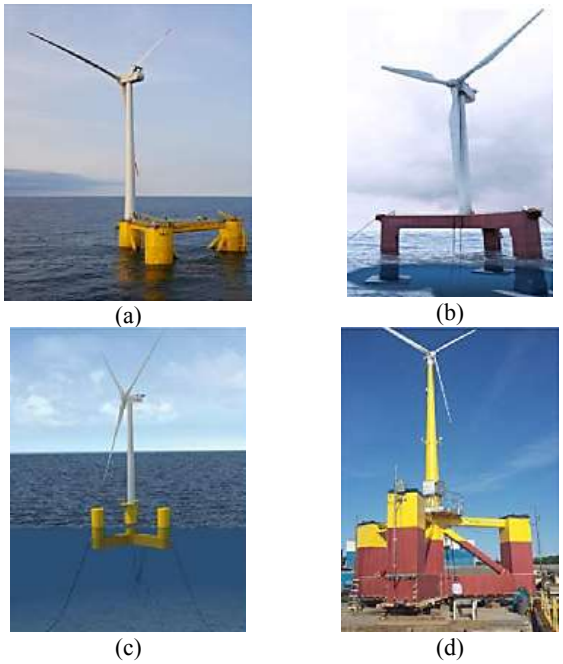

(a) (b) (c) (d)

Figure 1. Semi-submersible concepts for floating offshore wind turbines: (a) WindFloat (Principle Power) (b) Tri-Floater (GustoMSC) (c) Naval Energies Technology (d)Maine University Technology [8]

The hydrodynamic, aerodynamic, or aero-hydro-servo analysis of FOWTs has been the subject of numerous experimental and numerical studies. Benitez and his colleagues [9] studied the hydrodynamics of FOWTs by running numerical simulations on the semi-submersible platform DeepCwind in 2015 to find out how different geometric parameters affected the hydrodynamic coefficients. They specifically looked at drag behavior, free surface effects, and the multi-member configuration of the semi-submersible structure. Zhao and Wan [10] studied the hydrodynamic characteristics of the support platform displacements during wind turbine shutdown conditions utilizing OpenFOAM. The pitch and sway motion of the floating platform is affected by the aerodynamic loads from the turbine. In 2015, Dunbar [11] proposed a six DoF solver coupled with OpenFOAM for the excitation of semi-submersible floating offshore wind turbine platforms. The validation of the CFD simulation results for the DeepCwind semi-submersible platform was performed using experimental data across various sections, encompassing heave and pitch motions. In 2016, Yan and colleagues [12] proposed a computational framework using the finite element method with isogeometric analysis (IGA) to investigate fluid-structure interaction and assess the hydrodynamic forces on floating wind turbine platforms, with computational results validated against experimental data. In 2018, Wang and colleagues [13] conducted an extensive review of the diverse variables associated with offshore wind platforms in relation to specific sample projects, focusing particularly on a novel foundation for wind turbines. The researchers examined the system under diverse combined and extreme loads through numerical simulations and field tests, resulting in an enhanced geometric design that accounts for transportability. In 2020, Zhang and associates [14] performed a comparative analysis of the hydrodynamic performance of three platforms at varying water depths, taking into account second-order hydrodynamic forces. The pitch motion of the DeepCwind4 semi-submersible wind turbine is more responsive to second-order wave loads than the other two wind turbines. In 2021, Johalas and colleagues [15] investigated the performance of a 5 MW reference wind turbine installed on the semi-submersible platforms UMaine3OC and DeepCwind4OC under wind-wave conditions. The researchers analyzed the impact of the interaction between the movement of the support platform and the wind turbine rotor on the average power output, ultimately deriving a straightforward analytical formula for predicting average power in floating turbines at low wind speeds. In 2022, Wang and colleagues [16] conducted a study to validate the DeepCwind semi-submersible model

through computational fluid dynamics, which underwent free decay motion analysis. The researchers analyzed the hydrodynamic damping behavior and characteristics of the platform in calm water and validated their results with experimental data. In 2022, Serjinko and colleagues [17] published a review article analyzing various proposed techniques for advanced floating support structures designed for larger wind energy systems, emphasizing system dynamics. The findings indicated that the mass of the wind turbine, the rated power, and the rotor thrust scale correlate with the square of the rotor diameter. In 2022, Elkafas and colleagues [18] performed a numerical study on the hydrodynamic response of three distinct configurations of the DeepCwind model by altering the number of offset columns from three to five. Statistical findings concerning regular and irregular waves indicate that the wave response is inversely related to the quantity of offset columns. The effect of increasing offset columns on vertical displacements and elevation is minimal. In 2023, Eskilsson and associates [19] performed a numerical study simulating the hydrodynamics of the semi-submersible platform. The implementation of a one-way coupling in the mooring-fluid system yields marginally increased mooring forces, yet it does not substantially influence the motion response of the floating wind turbine. In 2024, Zhou and colleagues [20] investigated the hydrodynamic performance of a co-located farm comprising an array of OC4-DeepCwind FOWT and floating photovoltaic systems (FPVs). Case studies have been conducted to analyze the impact of platform geometric parameters on the hydrodynamic performance of wind and solar platforms. The results offer insights for the optimal design of floating photovoltaic systems and illustrate the potential synergy between wind and solar energy on floating platforms. In 2024, Zeng and colleagues [21] explored the theoretical challenges and progressed research developments associated with nonlinear hydrodynamic issues pertaining to floating offshore wind turbines (FOWT). They examined various nonlinear phenomena associated with their mooring systems, including low-frequency resonance, transient impacts, hydro-elastic coupling, flow effects, and shallow water effects, from both numerical and physical viewpoints. Numerous researchers have performed experimental investigations on FOWT [22, 23], including Chen and colleagues floating turbine model tests on various platforms [24], which assessed the distinctive relative performance of each of the three systems, focusing on structural motions, tower dynamics, and the system's heave response. In 2020, Belloli et al. [25] conducted a wind tunnel analysis of FOWT.

According to the literature review and the authors' expertise, the primary challenge for engineering teams designing these structures is the precise forecasting of the offshore platform's performance under all expected environmental conditions during its operational lifespan. Dynamic stability is the primary criterion for averting the capsizing or submersion of the offshore platform. Consequently, the imperative for additional research to ascertain an optimal solution that guarantees stability and efficiency at minimal expense is crucial. However, in order to analyze all the previously mentioned scenarios within a reasonable timeframe, researchers have consistently prioritized the creation of an engineering tool and a suitable study method based on simplified assumptions. This study examines the dynamic performance of the DeepCWind semi-submersible platform in freely floating conditions. This study aims to illustrate that the proposed method is effective, allowing for the utilization of numerical tools in place of laborious and complex FOWT simulations. The open-source CFD software OpenFOAM has been utilized for simulation to attain this objective, and the findings have been presented in a comparative format.

2. Governing Equations

The current study utilized the open-source software OpenFOAM for computational fluid dynamics simulation. The software, proficient in resolving Reynolds-Averaged Navier-Stokes (RANS) equations, executes dynamic motion simulations within the InterDyMFoam solver. The governing equations are delineated as follows.

In the field of rigid body motion, the transitional movement of the floating body with mass m exposed to the external force fi is as follows:

$$m\frac{dv}{dt} = f \tag{1}$$

where, v shows the velocity of the center of floating mass. Also, the equation of angular motions of a floating body around the center of mass has the following form:

$$M\frac{d\omega}{dt} + \omega \times M\omega = n \tag{2}$$

where, M is the tensor of moment of inertia, ω is the rigid body angular velocity, and n is the excitation force applied to the floating body. In order to dynamic analysis of sandglass, preliminary, according to fluid flow solution and pressure distribution on the submerged surface of the sandglass, excitation forces in Eq. (1 and 2) are derived. Then, body transitional and angular movements are derived by using Eq. (1 and 2). To this accomplishment, fluid flow is simulated by RANS equations. The free surface is also modeled by two-phase approach of fluid volume fraction and artificial density [26]. The conservation of mass and momentum equations in the two-phase fluid motion are as follows:

$$\nabla . U = 0 \tag{3}$$

$$\frac{\partial \rho U}{\partial t} + \nabla \cdot \left(\rho (U - U_g) U\right) = \quad (4)$$
$$-\nabla p_d - g \cdot \mathrm{x} \nabla \rho + \nabla \cdot \left(\mu_{eff} \nabla U\right) + (\nabla U) \cdot \nabla \mu_{eff} + f_\sigma$$

here, U and $\underline{U_g}$ are fluid velocity and grid cell movement velocity, respectively. Moreover, P_d is the dynamic pressure may be computed as $p_d = p - \rho g \cdot x$ (i.e. the difference between total and hydrostatic pressure). The acceleration of gravity is considered *as* $g = (0,0,-9.81)$. Effective dynamic viscosity is also equal with $\mu_{eff} = \rho(v + v_t)$ (i.e., where v_t and v are eddy and kinematic viscosities, respectively), and f_σ is the surface tension as a source term. The approach of fluid volume fraction is a method to estimate the free surface by using:

$$\frac{\partial \alpha}{dt} + \nabla \cdot \left[(U - U_g)\alpha\right] + \nabla \cdot \left[U_r (1-\alpha)\alpha\right] = 0 \quad (5)$$

here, the volume ratio (α) in the Eq.(5) is the properties of the fluid inside each cell as follows:

$$\begin{cases} \alpha = 0 & air \\ \alpha = 0 & water \\ 0 < \alpha < 1 & \text{int } erface \end{cases} \quad (6)$$

The variable U_r in Eq.(5) is the fluid domain velocity which applies the effects of velocity at the boundary of water and air [27]. It is notable that, the surface tension f_σ in Eq (4) is equal $f_\sigma = \sigma k \nabla \alpha$ (i.e., where k is the curvature of the free surface and σ = 0.07 kg/sq.s is the surface tension of water, which can be derived using the definition of volume ratio (α). Therefore, the density and dynamic viscosity of free surface is as follows:

$$\begin{cases} \rho = \alpha \rho_1 + (1-\alpha)\rho_g \\ \mu = \alpha \mu_1 + (1-\alpha)\mu_g \end{cases} \quad (7)$$

It is notable that the shear stress transport (SST) equation is also considered for the simulation of turbulent flow [28].

3. Physics of the Problem and Validation

As the main goal of this study is to analyze the dynamic behavior of offshore floating platforms, it is essential to assess the accuracy of the numerical solution method in comparison to experimental laboratory data. Consequently, prior to examining the calculations, a validation of the dynamic movements of a sand-glass type floating body (STFB) within floating production, storage, and offloading (FPSO) structures has been conducted. Figure 3 presents an illustration of the two-dimensional perspective and geometric characteristics of the STFB. This study presents the dynamic behavior of the STFB floating platform model at a 1:70 scale to evaluate the accuracy of the results obtained through the finite volume method, in comparison with other experimental [29] and numerical data. [30]. Table 1 presents the main physical parameters of the STFB.

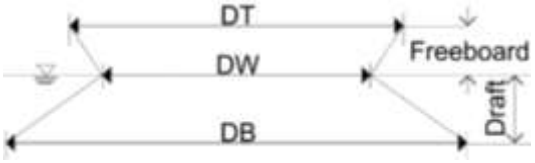

Figure 2. 2D section of STFB

Table 1. Main physical characteristics of considered STFBs

Parameter	Exp.	Model	Unit
Scale (λ)	1	70	-
Diameter of upper deck (D_T)	78.864	1.126	m
Diameter of waterline plane (D_W)	52.4	0.748	m
Radius of lower bottom (D_B)	90.012	1.286	m
Draft (d)	13.168	0.188	m
Freeboard (f)	20	0.286	m
Displacement (Δ)	55000	0.16	ton
Pitch inertia radius	17.550	0.251	m

A numerical wave tank (NWT) has been utilized in OpenFOAM with the InterDyMFoam solver to examine the dynamics of STFB in regular waves. The numerical simulations applied the Reynolds-Averaged Navier-Stokes (RANS) equations using the computational fluid dynamics (CFD) technique and resolved them using the FVM. The initial dimensions of the computational domain are L = 34 meters, B = 10 meters, and H = 14 meters, under deep water assumptions. The dimensions of the computational domain, as per ITTC guidelines for numerical methods and other dynamic analyses [31], are illustrated in Figure 4 for floating platforms. Figure 3 also illustrates the morphology of the mesh structure around the hull. A structural mesh has been employed in all solution domains, except in the regions surrounding the body, where multiple layers of graded structural and non-structural cells have been utilized.

The simulated periodic waves are classified as second-order Stokes waves. Harmonic waves are produced at the inlet boundary x = 10 by virtual alterations in horizontal velocity (i.e., the position of the wave generator), and the resultant regular wave propagates in the negative X direction. On the opposing side, where x = -24 meters, outlet conditions are applied. The center of mass of the STFB is positioned at x = 2.83 meters, utilizing the symmetry condition for the x = 0 plane.

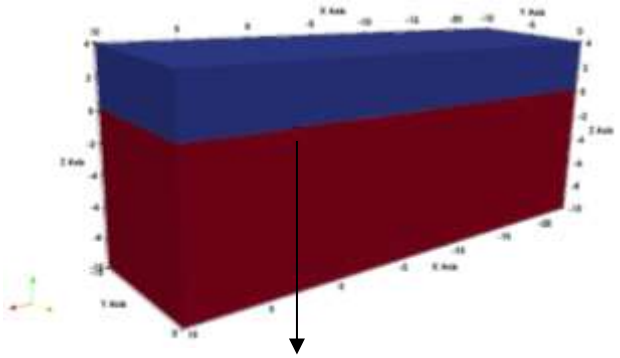

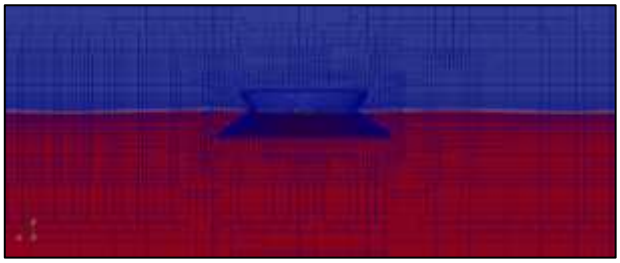

Figure 3. Considered numerical domain and the mesh structure around the STFB.

To validate the uncertainty in the numerical solution, three distinct mesh configurations, A, B, and C, have been evaluated for result accuracy. The numerical findings of this study regarding the heave of the STFB at a frequency of 0.29 have been analyzed using three distinct meshes. Table 2 presents the average values of the heave motion response for each cases. The mesh sensitivity analysis indicated that the total number of cells generated in the solution domain was approximately 1,181,169. This number has also been partially derived from wave characteristics. Due to the geometric characteristics of the model, the symmetry condition was applied to half of the computational domain. Then, the results are generalized for the entire computational domain.

Figures 4 and 5 illustrate the responses for heave RAO and pitch RAO of the STFB, simulated in this study with the FVM, in conjunction with experimental data [29], Boundary Element Method (BEM) results [32], and Boundary Value Problem (BVP) outcomes derived from WAMIT [29]. The current study's simulation demonstrates superior accuracy in both the magnitude and trend of the heave and pitch RAOs compared to the boundary element method and boundary value problem results.

Table 2. Details of mesh sensitivity analysis

Case	Δx [m]	Δy [m]	Δz [m]	Total cells	Run time	Mean value of Heave RAO [-]
A	0.012	0.012	0.012	524633	10 h	1.411
B	0.010	0.010	0.010	1012850	16 h	1.462
C	0.008	0.008	0.008	1485162	22 h	1.470

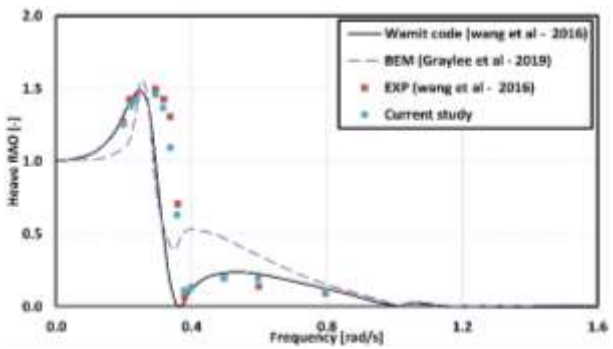

Figure 4. Heave RAO results of STFB

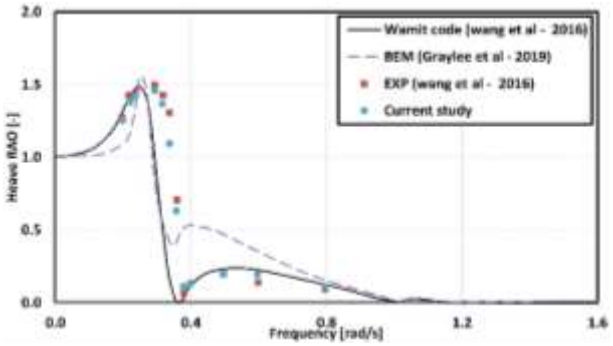

Figure 5. Pitch RAO results of STFB

Tables 3 and 4 present the quantitative discrepancies between the numerical results and the experimental data for the heave and pitch RAOs for each of the wave frequencies in this study. The assessment of the average error rate indicates that the finite volume method is an effective and dependable instrument for analyzing the dynamics of a floating platform in regular waves. The finite volume method has demonstrated a commendable capacity to accurately estimate the trends and recorded values of the floating platform's movements, particularly at critical points.

Table 3. Details of heave RAO compared to the experiment

Frequency [rad/s]	Heave RAO		
	Experimental data [29]	Current study	Error [%]
0.2	1.29	1.26	2.33
0.22	1.44	1.39	2.99
0.24	1.44	1.42	1.93
0.29	1.51	1.46	3.27
0.32	1.44	1.40	2.84
0.34	1.32	1.25	4.88
0.36	0.71	0.68	3.91
0.38	0.08	0.09	16.54
0.40	0.14	0.12	14.86
0.50	0.21	0.20	4.11
0.60	0.14	0.19	31.15
0.80	0.11	0.11	3.96

Table 4. Details of pitch RAO compared to the experiment

Frequency [rad/s]	Pitch RAO		
	Experimental data [29]	Current study	Error [%]
0.24	0.27	0.22	18.07
0.26	0.37	0.28	23.94
0.38	0.52	0.59	13.48
0.40	0.67	0.65	3.59
0.50	0.87	0.84	3.47
0.60	0.91	0.95	3.96
0.69	0.91	0.98	7.92
0.8	0.78	0.81	3.86

Linearized methods are predicted to exhibit considerable discrepancies when compared to experimental results. Consequently, when the objective of the research is to enhance the dynamic behavior of a complex or optimized geometric shape, linearized methods prove to be unreliable. Small deviations in the results are significant concerning the limitations of these methods.

4. Results and Discussion

This section models the DeepCWind concept for the dynamic analysis of the support platform bases subjected to regular waves. The OC4 and OC5 projects conducted testing campaigns for this design at a marine model scale of 1/50. Figure 6 illustrates that the DeepCWind semi-submersible platform comprises three offset columns (consisting of base and upper columns), a central column, and multiple sets of pontoons and cross braces.

Reference [22] details the platform movements and mooring system under wave-only or combined wave and wind conditions. This section presents simulations of the offset semi-submersible DeepCWind bases under free-floating conditions (without mooring) across various scenarios, based on the validation of the solution method and the accuracy of dynamic results in evaluating a floating platform. The primary physical characteristics of the reference platform are detailed in Table 5.

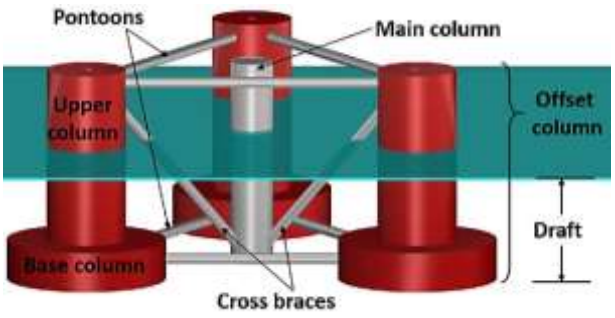

Figure 6. DeepCWind semi-submersible platform

Table 5. Characteristics of the main and the scaled models

Geometrical Characteristics	Exp.	Model
scale [-]	1	50
overall draft [m]	20	0.4
Main column (tower bottom) height above SWL [m]	10	0.2
Offset column height above SWL [m]	12	0.24
Distance among the offset columns [m]	50	1
Top columns length	26	0.52
Base columns length [m]	6	0.12
Distance up top of base columns under SWL [m]	14	0.28
Main columns diameter [m]	6.5	0.13
upper columns diameter [m]	1.2	0.024
Base columns diameter [m]	24	0.48
Cross braces and pontoon diameter [m]	1.6	0.032
Structural Characteristics		
Displacement [m^3]	13986.8	0.112
Center of mass (CM) location below SWL [m]	14.4	0.288
Platform pitch inertia about CM [kg-m^2]	8.01×10^9	25.64
Platform pitch inertia about CM [kg-m^2]	8.01×10^9	25.64
Platform Yaw inertia about platform centerline [kg-m^2]	13.9×10^9	44.51

This study excludes pontoons and cross braces. The simplified geometric configuration of the DeepCWind semi-submersible support platform has been employed to assess its dynamic behavior. The assessment of the two heave modes, reduced (wide) and increased (tight), of the offset bases relative to the original condition in free-floating wave scenarios has been performed. The reference support platform is depicted in three distinct configurations according to Figure 7. A refined state has been implemented to decrease the distance between the offset bases by 20%, while an expanded state has been adopted to increase the distance between the offset bases by 20% relative to the original state. The adjusted distance between the offset bases concerning the platform's center of buoyancy has been implemented. Furthermore, in conjunction with the three delineated models (refer to Figure 7), the dynamic outcomes of one of the platform's foundations (mono-offset column) are also exhibited. The semi-submersible platform models depicted in Figure 7 are incorporated in a comparative analysis to investigate the flow between the offset bases and its effect on the dynamic behavior of the supporting platform.

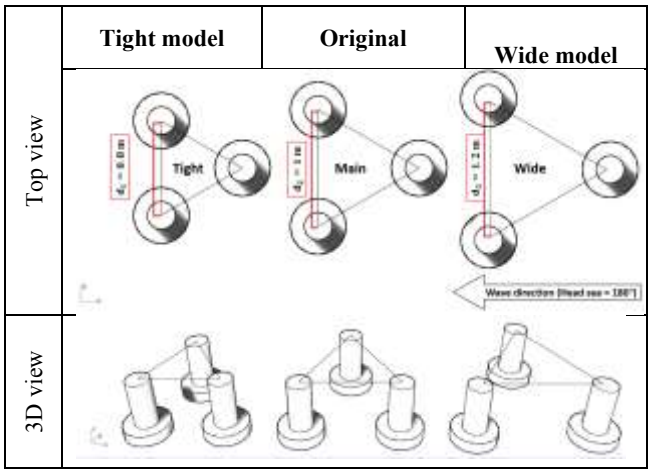

Figure 7. Diagram illustrating the specifications of three semi-submersible platform models: tight, original, and wide model determined by the distances between the offset bases

Figures 8 and 9 present the current study's free-floating condition results against the laboratory results constrained by the DeepCWind semi-submersible platform's mooring system. A comparative analysis of the heave and pitch motions of the platform across varying wave periods has been conducted, with the

horizontal and vertical axes denoting the wave impact periods (spanning from a wavelength of 0.5 to 21 meters) and the response amplitude operator (RAO), respectively. Figures 8 and 9 illustrate the impact of mooring on the amplitude response of the supporting platform's movements. The analysis of the motion curve's slope and the fluctuations in the platform's oscillations in a free-floating state, in comparison to the experimental data of Coulling et al. [22], suggests that the anchoring system is engineered to regulate pitch stability and diminish the amplitude of the platform's vertical oscillations. The maximum amplitude of the platform's longitudinal pitch in a free-floating state was observed at a wave period of 18 seconds; however, upon the application of anchoring effects, the floating platform demonstrated a more consistent pitching motion. In the vertical displacement motion of the support platform, the anchoring effects have resulted in a gradual decrease in the rate of increase of the platform's vertical oscillations, transitioning from shorter wavelength waves to longer wavelength waves (i.e., period interval 14 to 18 seconds).

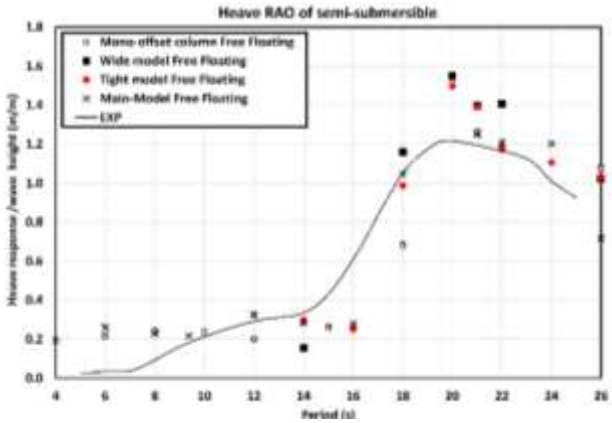

Figure 8. Comparison of heave RAO results of FOWT's platform in free-floating condition

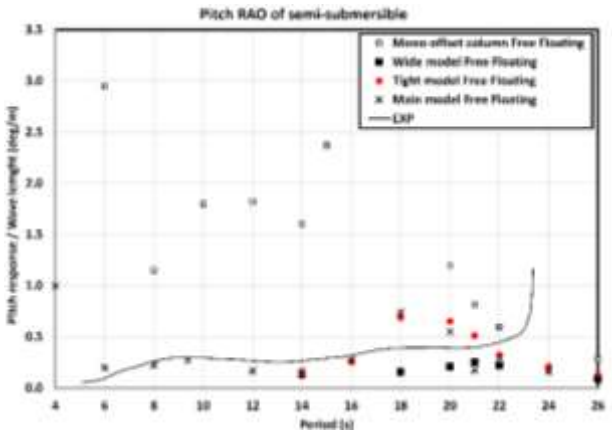

Figure 9. Comparison of pitch RAO results of FOWT's platform in free-floating condition

According to the observations in Figure 8, the primary model under free-floating conditions resembles that under anchored conditions for wave periods exceeding the critical range for certain resonances to manifest. The amplification of the platform's elevation movements at a period of 20 seconds may be attributed to the platform's increased submersion in water.

The dynamic outcomes of the wide and tight model have been analyzed solely within the critical range. Despite the negligible differences in results relative to the original state, discerning the dynamic behavior under various conditions yields valuable insights for the conceptual design of floating wind turbines. The picture in Figure 9 shows that the large semi-submersible platform model has decreased the pitch amplitude at most points within the critical range compared to the original model. However, it has increased the oscillations in heave motion for most wave periods compared to the original model. On the other hand, as shown in Figure 8, the small semi-submersible platform has effectively reduced the largest vertical displacement oscillations within the critical range of larger waves. It is noteworthy that in the pitch movement of the reduced-scale platform model, before the maximum dynamic response (wave period of 18 seconds), it displayed identical behavior to the original model. However, after reaching the apex, the scaled-down platform's curve continued to decline, exhibiting increased fluctuations compared to the original model.

5. Conclusions

Exploring renewable energy sources is crucial for achieving sustainable development. Wind energy serves as an appealing clean alternative to fossil fuels. The offshore wind power sector is experiencing significant growth. Offshore wind turbines offer several benefits in comparison to onshore wind platforms, including higher wind speeds, more consistent airflow with reduced turbulence, and fewer aesthetic concerns. Unlike traditional onshore or fixed offshore wind turbines, a floating offshore wind turbine (FOWT) requires a supporting platform. In a FOWT system, the upper wind turbine is connected to a lower floating platform, and the movements of each component influence one another. The current study highlights the importance of understanding the dynamic behaviors of floating offshore wind turbine (FOWT) platforms, specifically the DeepCWind model, under varying column offsets. The open-source CFD code of OpenFOAM models the three columns of FOWT's platform with various column offsets and free-floating mono-offset columns to achieve this accomplishment. Numerical simulations are conducted using a 3D RANS-VOF model and under regular wavy conditions. Preliminary mesh sensitivity analysis is conducted, and the numerical results of the sandglass-type FOWT platform are validated with experimental data. The main results indicate that increasing the distance between the platform columns significantly reduces heave and pitch motions, thereby enhancing the platform's stability and efficiency in real sea conditions.

6. References

[1] Koutoudjian, G., Diniz, L., Cespedes, R., & UNDP, V. G. (2021). About IRENA The International Renewable Energy Agency (IRENA) is an intergovernmental organisation that supports countries in their transition to a sustainable energy future, and serves as the principal platform for international co-operation, a centre of excellence, and a repository of policy, technology, resource and financial knowledge on renewable energy. IRENA promotes the. *IRENA promotes the*, 24.

[2] Eia, U. S. (2016). Levelized cost and levelized avoided cost of new generation resources in the annual energy outlook 2016. *Washington DC, USA*.

[3] Cozzi, L., Gould, T., Bouckart, S., Crow, D., Kim, T. Y., McGlade, C., ... & Wetzel, D. (2020). World energy outlook 2020. Energy, 2019, 30.

[4] Liu, Y., Xiao, Q., Incecik, A., & Wan, D. C. (2016). Investigation of the effects of platform motion on the aerodynamics of a floating offshore wind turbine. *Journal of Hydrodynamics*, *28*(1), 95-101.

[5] Castro-Santos, L., & Diaz-Casas, V. (Eds.). (2016). *Floating offshore wind farms* (p. 204). Switzerland: Springer International Publishing.

[6] James, R., & Ros, M. C. (2015). Floating offshore wind: market and technology review. *The Carbon Trust*, *439*.

[7] Cermelli, C., Aubault, A., Roddier, D., & McCoy, T. (2010, May). Qualification of a semi-submersible floating foundation for multi-megawatt wind turbines. In *Offshore Technology Conference* (pp. OTC-20674). OTC.

[8] Pinguet, R. (2021). *Hydrodynamics of semi-submersible floater for offshore wind turbines in highly nonlinear waves using Computational Fluid Dynamics (CFD), and validation of overset meshing technique in a numerical wave tank* (Doctoral dissertation, Ecole Centrale Marseille).

[9] Benitz, M. A., Schmidt, D. P., Lackner, M. A., Stewart, G. M., Jonkman, J., & Robertson, A. (2015, May). Validation of hydrodynamic load models using CFD for the OC4-DeepCwind semisubmersible. In *International Conference on Offshore Mechanics and Arctic Engineering* (Vol. 56574, p. V009T09A037). American Society of Mechanical Engineers.

[10] Zhao, W., & Wan, D. (2015). Numerical study of interactions between phase II of OC4 wind turbine and its semi-submersible floating support system. *J. Ocean Wind Energy*, *2*(1), 45-53.

[11] Dunbar, A. J., Craven, B. A., & Paterson, E. G. (2015). Development and validation of a tightly coupled CFD/6-DOF solver for simulating floating offshore wind turbine platforms. *Ocean Engineering*, *110*, 98-105.

[12] Yan, J., Korobenko, A., Deng, X., & Bazilevs, Y. (2016). Computational free-surface fluid–structure interaction with application to floating offshore wind turbines. *Computers & Fluids*, *141*, 155-174.

[13] Wang, X., Zeng, X., Li, J., Yang, X., & Wang, H. (2018). A review on recent advancements of substructures for offshore wind turbines. *Energy conversion and management*, *158*, 103-119.

[14] Zhang, L., Shi, W., Karimirad, M., Michailides, C., & Jiang, Z. (2020). Second-order hydrodynamic effects on the response of three semisubmersible floating offshore wind turbines. *Ocean Engineering*, *207*, 107371.

[15] Johlas, H. M., Martínez-Tossas, L. A., Churchfield, M. J., Lackner, M. A., & Schmidt, D. P. (2021). Floating platform effects on power generation in spar and semisubmersible wind turbines. *Wind Energy*, *24*(8), 901-916.

[16] Wang, L., Robertson, A., Jonkman, J., Kim, J., Shen, Z. R., Koop, A., ... & Yu, K. (2022). OC6 phase Ia: CFD simulations of the free-decay motion of the DeepCwind semisubmersible. *Energies*, *15*(1), 389.

[17] Sergiienko, N. Y., Da Silva, L. S. P., Bachynski-Polić, E. E., Cazzolato, B. S., Arjomandi, M., & Ding, B. (2022). Review of scaling laws applied to floating offshore wind turbines. *Renewable and Sustainable Energy Reviews*, *162*, 112477.

[18] Elkafas, A. G., Ahmed, Y. M., & Elgohary, M. M. (2022). Hydrodynamic analysis of floating offshore wind turbine With different numbers of offset columns. *Marine Technology Society Journal*, *56*(2), 8-19.

[19] Eskilsson, C., Fernandez, G. V., Andersen, J., & Palm, J. (2023, June). Hydrodynamic simulations of a FOWT platform (1st FOWT comparative study) using openfoam coupled to moodycore. In *ISOPE International Ocean and Polar Engineering Conference* (pp. ISOPE-I). ISOPE.

[20] Zhu, K., Shi, H., Tao, J., Gong, H., Han, Z., & Cao, F. (2024). Analytical study on hydrodynamic performance of co-located offshore wind–solar farms. *Physics of Fluids*, *36*(1).

[21] Zeng, X., Shao, Y., Feng, X., Xu, K., Jin, R., & Li, H. (2024). Nonlinear hydrodynamics of floating offshore wind turbines: A review. *Renewable and Sustainable Energy Reviews*, *191*, 114092.

[22] Coulling, A. J., Goupee, A. J., Robertson, A. N., Jonkman, J. M., & Dagher, H. J. (2013). Validation of a FAST semi-submersible floating wind turbine numerical model with DeepCwind test data. *Journal of Renewable and Sustainable Energy*, *5*(2).

[23] Chen, C., Ma, Y., & Fan, T. (2022). Review of model experimental methods focusing on

aerodynamic simulation of floating offshore wind turbines. *Renewable and Sustainable Energy Reviews*, *157*, 112036.

[24] Koo, B. J., Goupee, A. J., Kimball, R. W., & Lambrakos, K. F. (2014). Model tests for a floating wind turbine on three different floaters. *Journal of Offshore Mechanics and Arctic Engineering*, *136*(2), 020907.

[25] Belloli, M., Bayati, I., Facchinetti, A., Fontanella, A., Giberti, H., La Mura, F., ... & Zasso, A. (2020). A hybrid methodology for wind tunnel testing of floating offshore wind turbines. *Ocean Engineering*, *210*, 107592.

[26] Rusche, H. (2002). Computational fluid dynamics of dispersed two-phase flow at high phase fractions. Ph. D. thesis, University of London.

[27] Berberović, E., van Hinsberg, N. P., Jakirlić, S., Roisman, I. V., & Tropea, C. (2009). Drop impact onto a liquid layer of finite thickness: Dynamics of the cavity evolution. Physical Review E—Statistical, Nonlinear, and Soft Matter Physics, 79(3), 036306.

[28] Menter, F. R. (2009). Review of the shear-stress transport turbulence model experience from an industrial perspective. International journal of computational fluid dynamics, 23(4), 305-316.

[29] Wang, W. H., Wang, L. L., Du, Y. Z., Yao, Y. X., & Huang, Y. (2016). Numerical and experimental analysis on motion performance of new sandglass-type floating body in waves. *Marine structures*, *46*, 56-77.

[30] Graylee, A., & Yousefifard, M. (2020). The effects of different cross sections on the hydrodynamic behaviour of sandglass-type FPSOs exposed to regular waves. *Journal of Marine Engineering & Technology*, *19*(4), 197-206.

[31] Yousefifard, M., & Nowruzi, H. (2024). Hydrodynamic performance of sandglass-type floating body with damping appendages. *Ocean Engineering*, *309*, 118579.

[32] Graylee, A., & Yousefifard, M. (2020). The effects of different cross sections on the hydrodynamic behaviour of sandglass-type FPSOs exposed to regular waves. *Journal of Marine Engineering & Technology*, *19*(4), 197-206.